Evidence of the Missing Baryons from the Kinematic Sunyaev-Zeldovich Effect in Planck Data

Carlos Hernández-Monteagudo,[1,*] Yin-Zhe Ma,[2,3] Francisco S. Kitaura,[4] Wenting Wang,[5] Ricardo Génova-Santos,[6,7] Juan Macías-Pérez,[8] and Diego Herranz[9]

[1]Centro de Estudios de Física del Cosmos de Aragón (CEFCA), Plaza San Juan 1, planta 2, E-44001 Teruel, Spain
[2]Astrophysics and Cosmology Research Unit, School of Chemistry and Physics, University of KwaZulu-Natal, Durban, South Africa
[3]Jodrell Bank Centre for Astrophysics, School of Physics and Astronomy, The University of Manchester, Manchester M13 9PL, United Kingdom
[4]Leibniz-Institut für Astrophysik Potsdam (AIP), An der Sternwarte 16, D-14482 Potsdam, Germany
[5]Institute for Computational Cosmology, University of Durham, South Road, Durham DH1 3LE, United Kingdom
[6]Instituto de Astrofísica de Canarias, C/Vía Láctea s/n, E-38205 La Laguna, Tenerife, Spain
[7]Departamento de Astrofísica, Universidad de La Laguna (ULL), E-38206 La Laguna, Tenerife, Spain
[8]Laboratoire de Physique Subatomique et Cosmologie, Université Grenoble-Alpes, CNRS/IN2P3, 53 rue des Martyrs, 38026 Grenoble Cedex, France
[9]Instituto de Física de Cantabria (CSIC-Universidad de Cantabria), Avenida de los Castros s/n, E-39005 Santander, Spain

(Received 18 April 2015; revised manuscript received 16 July 2015; published 3 November 2015)

We estimate the amount of the *missing baryons* detected by the Planck measurements of the cosmic microwave background in the direction of central galaxies (CGs) identified in the Sloan galaxy survey. The peculiar motion of the gas inside and around the CGs unveils values of the Thomson optical depth τ_T in the range 0.2–2 $\times 10^{-4}$, indicating that the regions probed around CGs contain roughly half of the total amount of baryons in the Universe at the epoch where the CGs are found. If baryons follow dark matter, the measured τ_T's are compatible with the detection of all of the baryons existing inside and around the CGs.

DOI: 10.1103/PhysRevLett.115.191301 PACS numbers: 98.70.Vc, 98.52.Eh, 98.62.Py, 98.65.Hb

Introduction.—The interplay between baryons and dark matter is a key problem in cosmology and galaxy formation. Understanding the distribution of baryonic and dark matter in galaxies, groups, and clusters of galaxies is an essential step towards the full picture of how these objects form and evolve. It is well known [1–3] that only about 10% of all baryons in the Universe reside in the form of stellar mass, while the other 90% resides in a diffuse, mostly undetected component—it would remain completely hidden if it were not for recent UV spectroscopic measurements of uncollapsed, diffuse gas in the direction of certain quasistellar objects (see, e.g., Refs. [4,5] and the references therein). Nowadays, there is an ongoing debate [6–11] on whether a significant fraction of the latter component is present in the circumgalactic medium around halos, or if instead most of the gas has been expelled or never accreted due to feedback processes like galactic winds or active galactic nuclei activity. This connects the *missing baryon* issue with the complex problems of feedback and galaxy formation. Certainly, a more complete census of the baryon distribution in the Universe would be of great relevance in this context.

The kinematic Sunyaev-Zeldovich effect (hereafter, kSZ [12]) describes the Doppler shift in frequency induced in photons of the cosmic microwave background (hereafter, CMB) photons after they scatter off free electrons. This Thomson scattering induces frequency independent brightness temperature anisotropies in the CMB, which are given by [13]

$$\delta T_{\mathrm{kSZ}}(\hat{\mathrm{n}}) = -T_0 \int dl \sigma_T n_e \left(\frac{\mathbf{v}}{c}\cdot\hat{\mathrm{n}}\right) \simeq -T_0 \tau_T \left(\frac{\mathbf{v}}{c}\cdot\hat{\mathrm{n}}\right). \tag{1}$$

In this expression, the integral $\tau_T = \sigma_T \int dl n_e$ is conducted along the line of sight (LOS) given by $\hat{\mathrm{n}}$. We have made the approximation that the typical correlation length of LOS velocities (given by $\mathbf{v}\cdot\hat{\mathrm{n}}$) is much larger than the density correlation length, in such a way that the LOS velocity term may be pulled out of the kSZ integral. This is justified by the results of Planck Collaboration Int. XXXVII [14], who find a typical correlation length of peculiar velocities of 20–40 h^{-1} Mpc, well above the typical galaxy correlation length ($\sim 5\ h^{-1}$ Mpc). The expression above also shows that the kSZ constitutes an integral over the electron momentum, independently of the temperature, and thus counts *all* electrons in the bulk flows, regardless of whether they belong to collapsed structures or not.

Large scale, bulk matter flows were detected via the kSZ effect first by Ref. [15], and more recently by Ref. [14]. We build upon the latter work and extract physical constraints on the amount of baryons contributing to the kSZ signal and the implications of those measurements in the problem of the missing baryons. As in Ref. [14], we use the latest Planck data release (DR2) available at the Planck's Legacy Archive server [16], the central galaxy catalogue (hereafter, CGC) obtained from the Sloan Digital Sky Survey

SDSS/DR7 [17], and a mock catalogue of central galaxies obtained from the Millennium numerical simulation [18], to which we henceforth refer as the GALAXY mock catalogue. In this work we quote results for the Planck SEVEM CMB map, although similar results are obtained for all of the other cleaning algorithms. Our estimates of the kSZ temperature of Eq. (1) are taken from Ref. [14] and are obtained after applying aperture photometry (hereafter, AP) in the direction of the CGC members. We defer the reader to that paper for a more detailed description of the data under use, and a deeper discussion on the measurements of the kSZ, while in this Letter we concentrate upon the physical interpretation of such measurements. In particular, we set constraints on τ_T and the missing baryons from our AP measurements of δT_{kSZ} in Eq. (1).

Methodology and results.—The two statistics presented in Ref. [14] yielding kSZ evidence are the kSZ pairwise peculiar momentum [hereafter, $p_{\mathrm{kSZ}}(r)$] and the cross-correlation function of the kSZ temperature and the recovered radial peculiar velocity [hereafter, $w^{\delta T v^{\mathrm{rec}}}(r)$]. The $p_{\mathrm{kSZ}}(r)$ reflects the gravitational infall in pairs of galaxies and is computed from the sum

$$\hat{p}_{\mathrm{kSZ}}(r) = -\frac{\sum_{i<j}(\delta T_i - \delta T_j)c_{i,j}}{\sum_{i<j}c_{i,j}^2}, \tag{2}$$

where the weights $c_{i,j}$ are given by [19]

$$c_{i,j} = \hat{\mathbf{r}}_{i,j}\cdot\frac{\hat{\mathbf{r}}_i + \hat{\mathbf{r}}_j}{2} = \frac{(r_i - r_j)(1+\cos\theta)}{2\sqrt{r_i^2 + r_j^2 - 2r_i r_j\cos\theta}}. \tag{3}$$

Following the convention of Ref. [15], in this equation $\mathbf{r}_i$ and $\mathbf{r}_j$ are the vectors pointing to the positions of the ith and jth galaxies on the celestial sphere, r_i and r_j are the comoving distances to those objects, and $\mathbf{r}_{i,j} = \mathbf{r}_i - \mathbf{r}_j$ refers to the distance vector for this pair of galaxies. The hat symbol ($\hat{\mathbf{r}}$) denotes a unit vector in the direction of $\mathbf{r}$, and θ is the angle separating $\hat{\mathbf{r}}_i$ and $\hat{\mathbf{r}}_j$. Note as well that $\hat{\mathbf{r}}_{i,j}$ refers to the direction of the difference vector, i.e., $(\mathbf{r}_i - \mathbf{r}_j)/|\mathbf{r}_i - \mathbf{r}_j|$. On the other hand, the $w^{\delta T v^{\mathrm{rec}}}(r)$ function is computed as the spatial correlation function between the measured kSZ temperature estimates and the linear theory predictions of the radial peculiar velocity of the CGs (v^{rec}), $w^{\delta T v^{\mathrm{rec}}}(r) = \sum_{i,j}(\delta T_i v_j^{\mathrm{rec}} w_i w_j)/\sum_{i,j} w_i w_j$, where as before the i, j subindices refer to CGs and w_i, w_j to their weights. For both statistics, the δT_j's correspond to the AP estimates of the kSZ fluctuations of Eq. (1). We refer again to Ref. [14] for details on how linear theory predictions of CG radial peculiar velocities are obtained. Figure 1 displays the measured $p_{\mathrm{kSZ}}(r)$ and $w^{\delta T v^{\mathrm{rec}}}(r)$ functions under 5, 8, and 12 arcmin aperture radii for the SEVEM clean map of Planck (very similar estimates are found for other CMB clean maps). In order to estimate the amount of free electrons giving rise to these signals, we compare these measurements with predictions obtained from (i) the GALAXY mock catalogue of central galaxies, and (ii) a suite of 100 Gaussian simulations of the matter density contrast field that is then inverted into a peculiar velocity field by means of the linearized continuity equation. The Gaussian simulations of the density contrast are generated from a dark matter linear power spectrum compatible with Planck's cosmology, and they have no power at wave numbers $k > 0.15\ h\,\mathrm{Mpc}^{-1}$ since those are regarded as nonlinear scales. The first approach provides velocities for the halos hosting the CGs, while the second computes an estimate of the smooth, linear peculiar velocity in a region surrounding each CG. Following the approximation in Eq. (1), the green curves in Fig. 1 provide predictions for $p_{\mathrm{kSZ}}(r)$ and $w^{\delta T v^{\mathrm{rec}}}(r)$ from the GALAXY mock (the solid lines) and the Gaussian simulations (the dash-dotted lines), with a choice of $\tau_T = 5\times10^{-5}$ for display purposes. We find that, while for $w^{\delta T v^{\mathrm{rec}}}(r)$ the two predictions just differ in a ~15% amplitude factor, for $p_{\mathrm{kSZ}}(r)$ they differ both in shape and amplitude. Since the kSZ is built upon all electrons present in the volume sampled by the aperture photometry—and not necessarily bound to the CGs—we expect the real signal to lie between the two predictions.

Following the template fit approach used in Ref. [14] that conducts minimum χ^2 fits of the data to the predictions while assuming Gaussian and correlated errors, we obtain the density probabilities for τ_T as given in Fig. 2. When fitting to the predictions inferred from the GALAXY catalogue, we obtain τ_T estimates from $p_{\mathrm{kSZ}}(r)$ measurements falling in the $(0.1\text{–}1.1)\times10^{-4}$ range, in slight tension (between 1σ and 2σ low) compared to estimates from

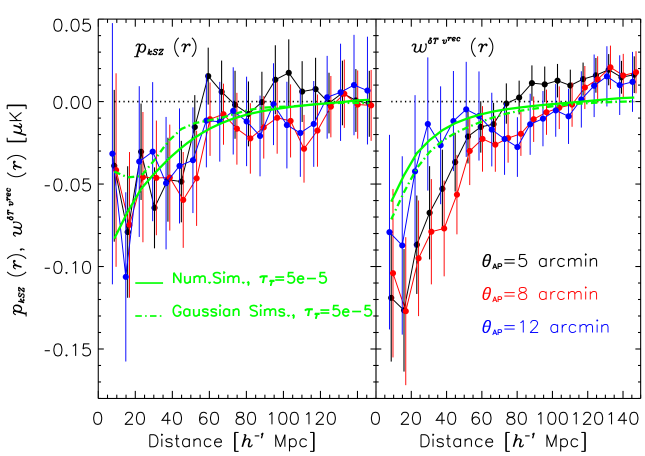

FIG. 1 (color online). (Left panel) Measured pairwise peculiar momenta under different aperture sizes for the SEVEM map. (Right panel) Measured $w^{\delta T v^{\mathrm{rec}}}(r)$ correlation function under different aperture radii (θ_{AP}) for the SEVEM clean map. In both panels the green solid lines provide the expectation from the GALAXY mock catalogue, while the dash-dotted lines correspond to expectations found after averaging over 100 Gaussian simulations. In both cases, we assume $\tau_T = 5\times10^{-5}$.

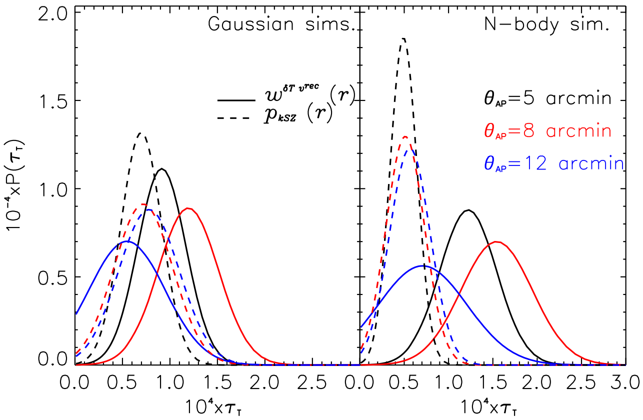

FIG. 2 (color online). (Left panel) Probability distribution for the optical depth τ_T inferred from the $w^{\delta T v^{\rm rec}}(r)$ correlation function (the solid lines) and the kSZ peculiar momenta (the dashed lines), under different apertures, for the SEVEM map. These estimates of τ_T are obtained after fitting the data to the prediction inferred from the average of the Gaussian simulations. (Right panel) Same as the left panel, but using the GALAXY N-body prediction as a reference, rather than the Gaussian simulations.

$w^{\delta T v^{\rm rec}}(r)$. A better consistency among τ_T estimates is found when fitting to the predictions provided by the Gaussian simulations (see the left panel of Fig. 2). The $p_{\rm kSZ}(r)$ and $w^{\delta T v^{\rm rec}}(r)$ measurements should yield similar τ_T estimates, and hence Fig. 2 suggests that the motion of electrons in and around CGs is better described by the Gaussian simulations, which we adopt in subsequent analyses. Note that this choice is not crucial for our discussion below.

We next estimate the baryon fraction giving rise to the observed τ_T amplitudes under different apertures. For any line of sight throughout any CG, all electrons inside a cylinder whose base radius is given by the angular aperture ($\theta_{\rm AP}$) should contribute to the signal. The LOS depth of this cylinder corresponds to the comoving length of typical velocity correlation ($L_{\rm corr}$), and it is suggested by Fig. 1 to lie in the 20–40 h^{-1} Mpc range (comoving units). We find, however, that the baryon fraction should not depend upon $L_{\rm corr}$ for any given aperture:

$$\langle f_b\rangle_z(\theta_{\rm AP}) = \left\langle \frac{\tau_T(\theta_{\rm AP},z)/(\sigma_T\bar{n}_e(z)L_{\rm corr}/(1+z))}{1/f_{\rm vol}(z)}\right\rangle_z$$
$$\approx \pi\frac{\langle\tau_T(\theta_{\rm AP},z)\rangle_z}{\sigma_T\bar{n}_{e,0}}\theta_{\rm AP}^2\langle n_{\rm CG}(z)d_A^2(z)\rangle_z, \qquad (4)$$

where $f_{\rm vol}(z)\simeq n_{\rm CG}(z)\pi(r(z)\theta_{\rm AP})^2L_{\rm corr}$ is the fraction of the comoving volume sampled by cylinders centered upon CGs, $L_{\rm corr}$ is the LOS depth of the cylinder in comoving units, $\bar{n}_e(z)$ is the average physical electron number density at redshift z (whereas the 0 subscript denotes the number density at present), $n_{\rm CG}(z)$ is the CG comoving number density, and $r(z)$ and $d_A(z)$ are the comoving and angular distances to redshift z, respectively. The brackets $\langle\ldots\rangle_z$ denote redshift averages, and thus our previous measurements of τ_T correspond to $\tau_T(\theta_{\rm AP}) = \langle\tau_T(\theta_{\rm AP},z)\rangle_z$. Note that Eq. (4) holds as long as there is no overlap between cylinders along two different LOSs: we have verified that such an overlap is negligible for apertures smaller than 13 arcmin, (it affects less than 1% of pairs falling in the first distance bin at ~9 h^{-1} Mpc, and this ratio is still smaller for the other distance bins). We remark that this definition of the baryon fraction computes the ratio of detected baryons around CGs to the *total* amount of baryons. Equation (4) shows that this baryon fraction depends on the CGC completeness via the product of the average CG number density times the average τ_T measured in and around those galaxies.

The top panel of Fig. 3 shows that the baryon fraction increases with the aperture, amounting to 45%–55% of the total of all baryons for $\theta_{\rm AP}\sim 8$–10 arcmin. For larger apertures, our measurements become compatible with noise and oscillate around zero. The blue lines provide the prediction for a scenario where the baryons trace perfectly the distribution of dark matter. These predictions follow the approach of Ref. [20], which computes the dark matter–central halo correlation function $\xi_{h,m}(r)(\propto\delta\rho_m(r))$. This is dependent on both the mass and the redshift of the halos and requires some linear bias relation $b(M,z)$, which we adopt from Ref. [21]. These predictions compute, as in Eq. (4), the ratio between the mean dark matter overdensity inside the cosmological volume sampled by the cylinders centered upon the CGs and the inverse of the fraction of the total cosmological volume sampled by the same cylinders. We thus need to integrate $\xi_{h,m}(r)$ inside the cylinders, and as shown in the plot these predictions are independent of the choice of $L_{\rm corr}$. We can also incorporate the impact of our AP filter in our prediction, after taking into account the redshift and the mass distribution of our CG sample for each aperture $\theta_{\rm AP}$. We find that our measurements of the baryon fraction are compatible with this prediction, although falling slightly on the high amplitude side: results from $w^{\delta T v^{\rm rec}}(r)$ are given by the filled red circles (filled green squares) when positive (negative), while the filled red triangles (empty green triangles) correspond to positive (negative) f_b estimates inferred from the $p_{\rm kSZ}(r)$. A template fit to the dark matter prediction [given by the blue lines and performed as in Eqs. (11) and (12) in Ref. [14], thus accounting for covariance among different apertures] yields an amplitude of $A_{\rm DM} = 1.15\pm 0.30$ for baryon fraction estimates obtained from the $w^{\delta T v^{\rm rec}}(r)$, and $A_{\rm DM} = 1.20\pm 0.22$ from the $p_{\rm kSZ}(r)$ measurements of the baryon fraction. In both cases we compare these observables to the prediction from Gaussian simulations. As mentioned above, tension at the 1.6σ level arises when comparing fits of the two $w^{\delta T v^{\rm rec}}(r)$, $p_{\rm kSZ}(r)$ observables to the N-body GALAXY prediction: $A_{\rm DM} = 1.49\pm 0.37$ vs $A_{\rm DM} = 0.85\pm 0.15$ from the $w^{\delta T v^{\rm rec}}(r)$ and $p_{\rm kSZ}(r)$ data, respectively. We remark that calibration errors in CMB maps would impact these amplitudes while leaving the significance of the kSZ signal unchanged.

Alternatively, in the bottom panel of Fig. 3, we compare the gas overdensity values inferred from the τ_T measurements from our $w^{\delta T v^{\rm rec}}(r)$ observations and $L_{\rm corr} = 38\ h^{-1}$ Mpc (the filled symbols) with the predictions of dark matter according to Ref. [20] (the blue dot-dashed line), for different choices $L_{\rm corr}$. In this case, the conversion between angular apertures and transversal distances accounts for the redshift distribution of the CG sources. Values for gas overdensity are obtained from $\tau_T(\theta_{\rm AP})$ estimates via

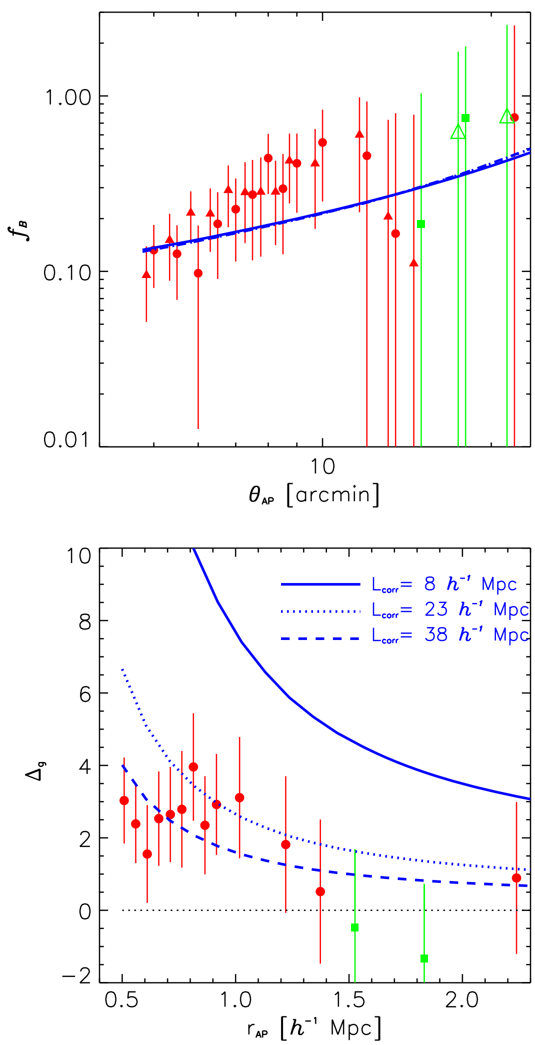

FIG. 3 (color online). (Top panel) Baryon fraction versus aperture angle, as inferred from $w^{\delta T v^{\rm rec}}(r)$ (the filled circles and squares) and $p_{\rm kSZ}(r)$ (the filled and empty triangles) measurements. Red (green) denotes positive (negative) values. (Bottom panel) Recovered profile of gas overdensity from $w^{\delta T v^{\rm rec}}(r)$ measurements and for $L_{\rm corr} = 38\ h^{-1}$ Mpc (the filled symbols). In both panels, we compare our data to the predictions for dark matter (as provided by Ref. [20]), which are given by the blue lines.

$$\Delta_g(r_{\rm AP}) \approx \frac{\langle \tau_T(\theta_{\rm AP}, z)\rangle_z}{\langle \sigma_T \bar{n}_e(z) L_{\rm corr}/(1+z)\rangle_z}. \qquad (5)$$

We again find good agreement with the dark matter prediction, finding no hint of the feedback that is supposed to deplete gas from the inner halo regions. Similar results are obtained from $p_{\rm kSZ}(r)$ observations.

Discussion.—Observations of metallic lines in the x ray in the direction of high energy sources provide information about the gas density in the so-called circumgalactic medium of the Milky Way [6,7,9,11]. While some authors claim to have found evidence for all of the baryons expected in our halo [6], some other authors seem to find only between 10% and 50% of the expected amount of baryons [7,9,11]. Both the thermal Sunyaev-Zeldovich (hereafter, tSZ [22]) and the kSZ effects provide alternative approaches to detect ionized gas, different from the window available from x-ray observations. The tSZ and kSZ effects provide statistical measurements of the gas fraction in the visible halo population and are not restricted to the Milky Way host halo. In Ref. [8] it is claimed that there is no apparent evidence for feedback effects in the tSZ luminosity of CGs, in contradiction to x-ray observations. Those analyses have been recently revisited by Ref. [10] after including explicitly the impact of feedback in the filters extracting the tSZ signal. They conclude that Planck tSZ observations up to $5R_{500}$ are compatible with active-galactic-nucleus-induced feedback effects, and incompatible with the no-feedback hypothesis (or self-similarity in the tSZ luminosity–halo mass relation). Those results restrict, however, to gas collapsed in halos that is able to generate a tSZ signal [23]. On the other hand, our kSZ study is blind to any assumed gas temperature profile in CG host halos, is not restricted to collapsed or virialized gas, and provides *lower* limits to the amount of gas in CGs given the compensated structure of the AP filter. Figure 3 shows that our measurements are compatible with having detected all missing baryons in a case where these follow the dark matter distribution. There exist uncertainties linked to the predictions for the gas peculiar velocities, but these are relatively small if we compare the predictions from the Millennium and Gaussian simulations in the right panel of Fig. 1. The impact of contaminants (such as dust or tSZ) seems to have been characterized and kept under control in Ref. [14], where it is also shown that a satellite fraction (of ∼12%) in our CGC should decrease the kSZ amplitude by less than 10%. We thus conclude that the measured kSZ signal provides evidence for all the missing baryons predicted to be inside and around the CGs, which correspond to roughly half the total amount of baryons present in the Universe at $z \simeq 0.12$ under the SDSS DR7 angular footprint. In the future, a more detailed comparison with state-of-the-art hydrodynamical numerical simulations should shed more light on these results.

C. H.-M. acknowledges the support of Ramón y Cajal Fellowship No. RyC-2011-08262, Marie Curie Career Integration Grant No. 294183, and Spanish Ministerio de Economía y Competitividad Project No. AYA2012-30789. We also acknowledge the useful discussions with S. D. M. White. Y.-Z. M thanks ERC for its support through Starting Grant No. 307209.

*chm_AT_cefca.es

[1] M. Fukugita and P. J. E. Peebles, Astrophys. J. **616**, 643 (2004).
[2] R. Cen and J. P. Ostriker, Astrophys. J. **650**, 560 (2006).
[3] J. N. Bregman, Annu. Rev. Astron. Astrophys. **45**, 221 (2007).
[4] J. M. Shull, B. D. Smith, and C. W. Danforth, Astrophys. J. **759**, 23 (2012).
[5] N. Tejos, S. L. Morris, C. W. Finn, N. H. M. Crighton, J. Bechtold, B. T. Jannuzi, J. Schaye, T. Theuns, G. Altay, O. Le Fèvre, E. Ryan-Weber, and R. Davé, Mon. Not. R. Astron. Soc. **437**, 2017 (2014).
[6] A. Gupta, S. Mathur, Y. Krongold, F. Nicastro, and M. Galeazzi, Astrophys. J. **756**, L8 (2012).
[7] A. Gatto, F. Fraternali, J. I. Read, F. Marinacci, H. Lux, and S. Walch, Mon. Not. R. Astron. Soc. **433**, 2749 (2013).
[8] P. A. R. Ade *et al.* (Planck Collaboration), Astron. Astrophys. **557**, A52 (2013).
[9] J. K. Werk, J. X. Prochaska, J. Tumlinson, M. S. Peeples, T. M. Tripp, A. J. Fox, N. Lehner, C. Thom, J. M. O'Meara, A. B. Ford, R. Bordoloi, N. Katz, N. Tejos, B. D. Oppenheimer, R. Davé, and D. H. Weinberg, Astrophys. J. **792**, 8 (2014).
[10] A. M. C. Le Brun, I. G. McCarthy, and J.-B. Melin, Mon. Not. R. Astron. Soc. **451**, 3868 (2015).
[11] M. J. Miller and J. N. Bregman, Astrophys. J. **800**, 14 (2015).
[12] R. A. Sunyaev and I. B. Zeldovich, Mon. Not. R. Astron. Soc. **190**, 413 (1980).
[13] R. A. Sunyaev and Y. B. Zeldovich, Astrophys. Space Sci. **7**, 3 (1970).
[14] P. A. R. Ade *et al.* (Planck Collaboration), arXiv:1504.03339 [Astron. Astrophys. (to be published)].
[15] N. Hand *et al.*, Phys. Rev. Lett. **109**, 041101 (2012).
[16] Planck's Legacy Archive: http://pla.esac.esa.int/pla/.
[17] K. N. Abazajian, J. K. Adelman-McCarthy, M. A. Agüeros, S. S. Allam, C. Allende Prieto, D. An, K. S. J. Anderson, S. F. Anderson, J. Annis, N. A. Bahcall *et al.*, Astrophys. J. Suppl. Ser. **182**, 543 (2009).
[18] V. Springel, S. D. M. White, A. Jenkins, C. S. Frenk, N. Yoshida, L. Gao, J. Navarro, R. Thacker, D. Croton, J. Helly, J. A. Peacock, S. Cole, P. Thomas, H. Couchman, A. Evrard, J. Colberg, and F. Pearce, Nature (London) **435**, 629 (2005).
[19] P. G. Ferreira, R. Juszkiewicz, H. A. Feldman, M. Davis, and A. H. Jaffe, Astrophys. J. Lett. **515**, L1 (1999).
[20] E. Hayashi and S. D. M. White, Mon. Not. R. Astron. Soc. **388**, 2 (2008).
[21] R. K. Sheth and G. Tormen, Mon. Not. R. Astron. Soc. **308**, 119 (1999).
[22] R. A. Sunyaev and Y. B. Zeldovich, Comments Astrophys. Space Phys. **4**, 173 (1972).
[23] C. Hernández-Monteagudo, H. Trac, L. Verde, and R. Jimenez, Astrophys. J. Lett. **652**, L1 (2006).